A Novel CMOS Optoelectronic Receiver IC for Elder-Care LiDAR Sensors

Ji-Eun Joo[1,2], Yu Hu[1,2], Myung-Jae Lee[3], and Sung Min Park[1,2,a]
[1]Department of Electronic and Electrical Engineering, Ewha Womans University
[2]Graduate Program in Smart Factory, Ewha Womans University
[3]Post-Silicon Semiconductor Institute, Korea Institute of Science and Technology
E-mail: [1,2]wxop01@naver.com, [1,2,a]smpark@ewha.ac.kr

***Abstract* -An optoelectronic receiver IC is presented for the applications of elder-care LiDAR sensors by utilizing a 180-nm CMOS technology, which consists of a spatially modulated P^+/N-well avalanche photodiode (APD), A2V (amplitude-to-voltage) converter exploiting inverter-type transimpedance amplifier, and T2V (time-to-voltage) converter, respectively. Simulation results reveal that the analog A2V circuit recovers 1.0 μA_{pp} ~ 1.1 mA_{pp} input currents with an almost linear step with the help of external gain control scheme, while the T2V circuit acquires 64.4 dB input dynamic range with a linear voltage step of 160 mV for each 10-ns time interval. The chip dissipates 4.1 mW from a single 1.8-V supply.**

***Keywords*—avalanche photodiode, current-mode, LiDAR, optoelectronic, TIA.**

I. INTRODUCTION

Recently, light detection and ranging (LiDAR) sensors have been popular in various applications such as unmanned autonomous vehicles, e.g., Google self-driving cars, remote sensing LiDAR sensors for observing forestry, cryosphere, aerosols, and clouds, and home-monitoring LiDAR sensors to help nurses or families to take care of senile dementia patients. Most LiDAR sensors exploit the pulsed time-of-flight (ToF) mechanism, so that light signals can be emitted from transmitter to targets located within a feasible range and its reflected light pulses can be detected by optical receiver. With the speed of light known, the target distance can be measured by the time difference between the transmitted (or START) pulse and its reflected (or STOP) pulse. Even for indoor home-monitoring sensor applications, the dynamic range of the received pulses (or echoes) should be wide, i.e., greater than 1:1,000, hence mandating fast response.

Meanwhile, the population of single seniors has become more than 20 percent in South Korea, which might cause serious social issues such as single elders, senile dementia patients, etc. In particular, they easily suffer declining cognitive ability and tend to face the dangers of falling accidents, heart attack during sleep, even suicide [1]. The Ministry of Health-Welfare predicted that one-million elders (10 % of senior citizens) might suffer dementia in 2025. Accordingly, the extremely high cost of two trillion won might have to be spent to treat some elders especially suffered from falling accidents. Also, the Alzheimer Nederland Foundation predicted that half a million elders (i.e., 13 % of senior citizens in Nederland) might suffer dementia in 2040 [2]. The government of Canada presented the statistics of falling accidents over 65 years old, showing that 50 % of the falling accidents occur mostly in houses, 60 % of these accidents are caused during walking, and the hospitalization rates related to these falling accidents increase rapidly for those over 65 years old [3]. Besides, single elders who live alone are afraid to experience sudden death from heart attack and many other illnesses. Even though some seniors live with their family, it is very hard to handle the situations of sudden death such as suicide. Hence, it is necessary for the sake of human dignity and keeping precious life to install sensors in their houses so that either their family or visiting nurses can recognize dangerous situations instantly after any kind of accidents at home. It is moreover desired that the sensors can detect the resting breath rate of elders in real-time, hence enabling to prevent rapidly sudden death or any other situation.

A monitoring sensor for the elders is required to be very small, invisibly equipped at a corner of a ceiling, and above all provide depth information in emergency, thus alarming the situations promptly to supervisors including family and nurses. For these purposes, a small, low-power, low-cost LiDAR sensor can be a feasible solution not only because its final images can be mostly blurred, thus avoiding portrait right violation, but also because it can precisely provide every necessary information of elders including move, falling, breath rate, etc. In addition, it can provide a number of advantages over conventional RF sensors due to their robustness against large RF interference [4,5].

Fig. 1 depicts the block diagram of a typical elder-care LiDAR sensor, where the transmitter (Tx) emits a light pulse to a target (a single elder in this figure).

a. Corresponding author; smpark@ewha.ac.kr

Manuscript Received Jun. 1, 2023, Revised Aug. 11, 2023, Accepted Aug. 17, 2023

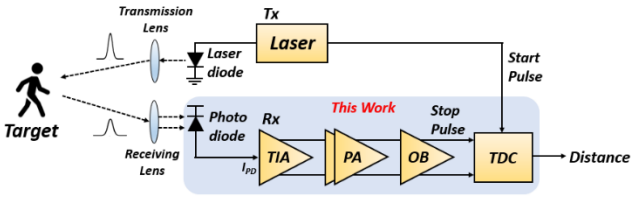

Fig. 1. Block diagram of a typical LiDAR sensor.

The reflected light pulse enters the optoelectronic receiver IC, which converts the light pulse into a digital code in the end, so that either the distance to the target or its depth information can be easily estimated. The 3D images of a targeted single elder can be achieved by utilizing FPGA-based verification process. Then, the images will be delivered to family/nurses in real-time, thus avoiding feasible dangerous outcome from falling and suicide. Meanwhile, CMOS on-chip avalanche photodiodes (APD) are very attractive because they can lower the total cost of multi-channel modules under the condition that the on-chip APD should yield appropriate optical responsivity.

Certainly, the wavelength of 850 nm is utilized for the CMOS silicon APD, and therefore it might be detrimental to eye-safety with large power emission. In this work, a CMOS optoelectronic receiver IC is presented for elder-care home-monitoring LiDAR sensors, which consist of a spatially modulated P$^+$/N-well APD, a voltage-mode CMOS feedforward transimpedance amplifier (VCF-TIA), an amplitude-to-voltage (A2V) converter, and a time-to-voltage (T2V) converter.

II. ARCHITECTURE

A. Circuit Description

Fig. 2 depicts the cross-sectional view and the layout of the P$^+$/N-well on-chip APD, as described in [6]. It blocks the part of active area using a metal layer to subtract slow diffusion currents of the photodetector. Therefore, the bandwidth is typically extended, however, at the expense of its responsivity [7].

Fig. 3 shows the block diagram of the optoelectronic Rx which consists of A2V and T2V, and the schematic diagram of the VCF-TIA that employs that comprises a conventional voltage-mode inverter (INV) input stage with a feedback resistor (R_F), a feedforward common-source amplifier with its gate connected to the gates of the INV stage.

According to the small signal analysis of the simplified feedforward input stage, the transimpedance gain is given by, (1)

$$Z_T(0) = -\frac{(g_{m1}+g_{m2}+g_{m3})R_F - 1}{g_{m1}+g_{m2}+g_{m3}+\dfrac{1}{r_{o1}||r_{o2}||r_{o3}||R_L}} \cong -R_F$$

The input-referred noise current spectral density is given by, (2)

$$\overline{I^2}_{n,TIA}(f) \cong \frac{4kT}{R_F} + 4kT\Gamma\left(\frac{1}{g_{m1}}+\frac{1}{g_{m2}}\right)\times\left[(2\pi C_T)^2 f^2 + \frac{1}{R_F^2}\right] + 4kT\left(\Gamma\frac{1}{g_{m3}}+R_G\right)\times\left[(2\pi C_T)^2 f^2 + \frac{1}{R_F^2}\right] \cong \frac{4kT}{R_F} + 4kT\Gamma\left(\frac{1}{g_{m1}}+\frac{1}{g_{m2}}+\frac{1}{g_{m3}}\right)\times(2\pi C_T)^2 f^2$$

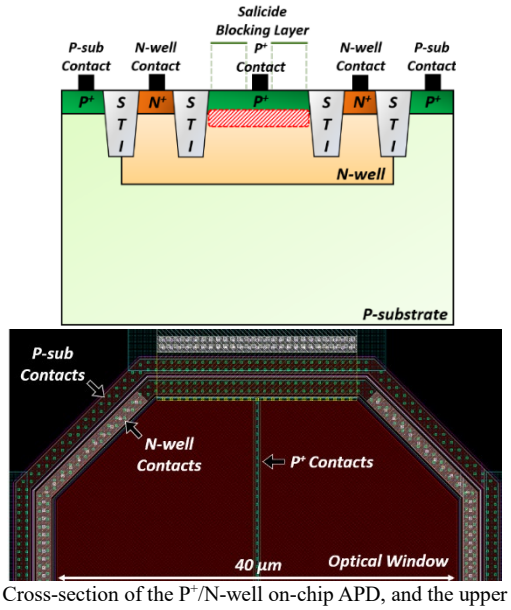

Fig. 2. Cross-section of the P$^+$/N-well on-chip APD, and the upper half of its layout.

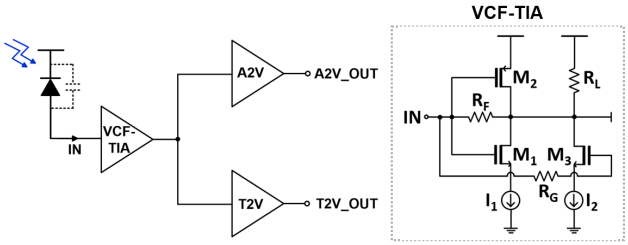

Fig. 3 Block diagram of the optoelectronic Rx IC.

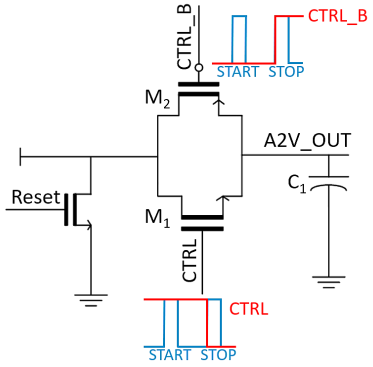

(a)

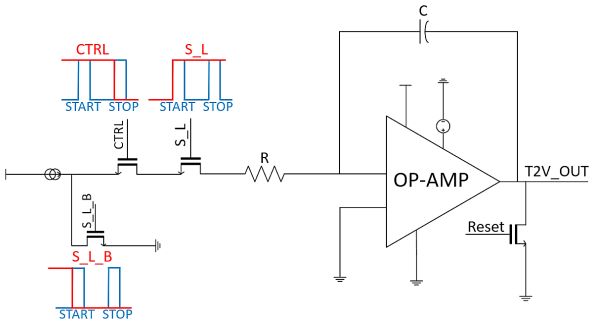

(b)

Fig. 4. Schematic diagrams of (a) A2V and (b) T2V.

, where k is the Boltzmann′s constant, T is the absolute temperature, and $\Gamma(\approx 2)$ is the Ogawa′s noise factor of a MOSFET. Furthermore, C_T $(= C_{PD} + C_{in,M1} + C_{in,M2})$ represents the total capacitance at the input node of the VCF-TIA which includes the photodiode capacitance (C_{PD}) and the input capacitance of the INV input stage, i.e., $C_{in,M1} + C_{in,M2} = C_{gs1} + C_{gs2} + (1 + A_v)(C_{gd1} + C_{gd2})$. It is noted that R_G is set to 1 kΩ in this work so that the noise contribution from R_G can be negligible.

Then, the input-referred mean-square noise current is given by,

$$\overline{i^2}_{n,TIA} \cong \frac{4kT}{R_F} BW_{n1} + \frac{4kT\Gamma}{3} C_T^2 BW_{n2}^2 \left(\frac{1}{g_{m1}} + \frac{1}{g_{m2}} + \frac{1}{g_{m3}}\right)$$

, where BW_{n1} is the noise bandwidth for white noise and BW_{n2} is the noise bandwidth for f^2 noise. For $Q = 1/\sqrt{2}$, $BW_{n1} \approx 1.11 \cdot BW^3_{3dB}$ and $BW_{n2} \approx 1.49 \cdot BW_{3dB}$ [8].

The value of R_L is selected to a few tens of kilo-ohm. Then, the bias current (I_2) of M_3 can be mostly supplied through the PMOS (M_2) of the INV stage, because the DC drain voltage of M_2 is fixed by the action of the INV stage via the feedback resistor (R_F). Hence, this action enables to boost the transconductance (g_{m2}) of M_2 and helps to reduce the noise current spectral density of the feedforward TIA.

Fig. 4 shows the schematic diagrams of the proposed A2V and T2V converters, in which the A2V circuit employs a sample and hold configuration to guarantee the limiting operations with an ideally infinite gain, while the T2V circuit exploits an integrator with an MIM capacitor to generate a linear relationship of time-interval with the output voltage.

B. Chip Layout & Post-Layout Simulation Results

Fig. 5 shows the layout of the proposed optoelectronic receiver IC, where the chip core occupies the area of 187 x 111 μm^2. Post-layout circuit simulations were conducted by utilizing a standard 180-nm CMOS process parameters.

Fig. 6 depicts the simulated transient response of the proposed A2V converter, recovering the input currents of 1 μA_{pp} ~ 1.1 mA_{pp} with gain control scheme.

Fig. 7 shows the simulated transient response of the proposed T2V converter, acquiring 64.4 dB input dynamic range with a linear voltage step of 160 mV for each 10-ns time interval, which corresponds to the minimum detection range of 3 cm and the maximum detection range of 15 meters.

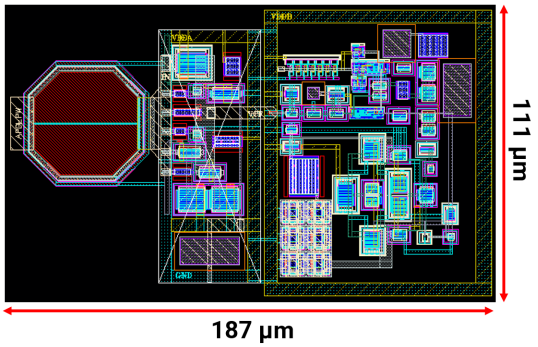

Fig. 5. Layout of the proposed optoelectronic receiver IC.

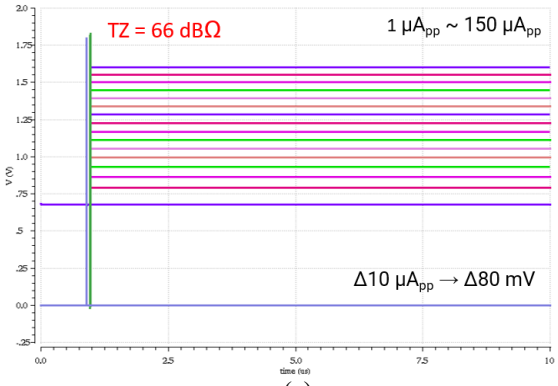

(a)

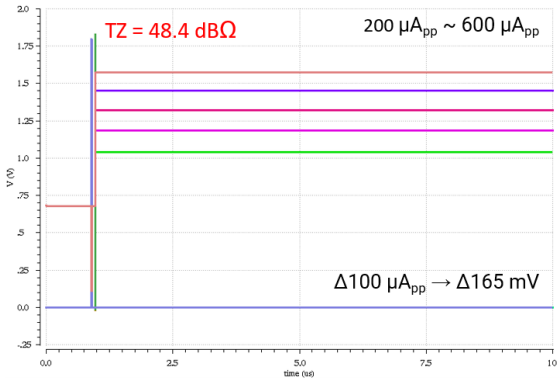

(b)

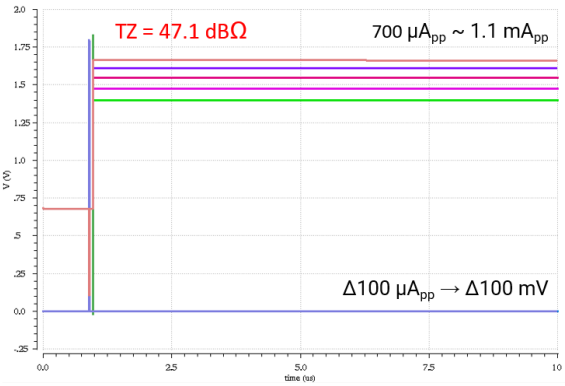

(c)

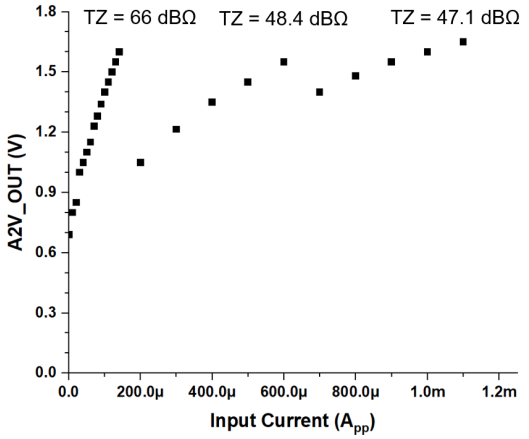

(d)

Fig. 6. Simulated A2V of the proposed optoelectronic receiver IC with different gain control for the input currents of (a) 1 ~ 150 μA_{pp}, (b) 200 ~ 600 μA_{pp}, (c) 0.7 ~ 1.1 mA_{pp}, respectively, and (d) the linearity plot of A2V.

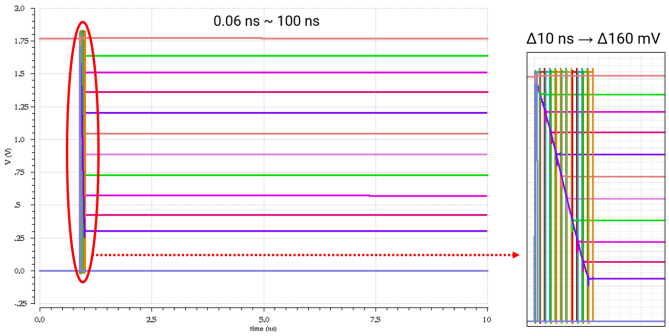

Fig. 7. Simulated T2V of the proposed optoelectronic receiver IC.

TABLE I. Performance Summary of the Proposed Optoelectronic Rx IC.

Parameters	This work
Supply Voltage	1.8 V
TZ Gain	64.4 dBΩ
Input current range	1.0 μA_{pp} ~ 1.1 mA_{pp}
Power dissipation per channel	4.1 mW
Core area	111 x 187 μm^2

Table I summarizes the performance of the proposed optoelectronic receiver IC that recovers both voltage amplitude and time interval with good linearity for the LiDAR applications. Furthermore, it was designed in low-power and small area, which helps to facilitate the implementation of multi-channel arrays.

III. Conclusions

We have suggested an optoelectronic receiver IC realized in a 180-nm CMOS technology for the applications of elder-care LiDAR sensors. It provides various advantages, such as lower cost, simpler integration, smaller package parasitic, etc. Conclusively, it is certain that this work enables to provide a potential for a low-cost sensor solution for short-range home-monitoring systems, especially to save single elders and/or dementia patients in cases of emergency.

Acknowledgment

This research was supported by the MSIT (Ministry of Science and ICT), Korea, under the ITRC (Information Technology Research Center) support program (IITP-2020-0-01847) supervised by the IITP (Institute for Information & Communications Technology Planning & Evaluation). Also, this work was supported by the National Research Foundation (NRF), Korea, under project BK21 FOUR. The EDA tool was supported by the IC Design Education Center.

References

[1] M. Montero-Odasso, J. Verghese, O. Beauchet, and J. M. Hausdorff, "Gait and Cognition: A Complementary Approach to Understanding Brain Function and the Risk of Falling," ***J. of American Geriatrics Society***, vol. 60, no. 11, pp. 2127–2136, Nov. 2012.

[2] B. D. Boer, J. Hamers, H. Beerens, S. Zwakhalen, F. Tan, and H. Verbeek, "Living at the farm, innovative nursing home care for people with dementia – study protocol of an observational longitudinal study," ***BMC Geriatrics***, vol. 15, no. 1, Feb. 2015.

[3] D. Yoon et al., "Mirrored Current-Conveyor Transimpedance Amplifier for Home Monitoring LiDAR Sensors," ***IEEE Sensors J.***, vol. 21, pp. 5589-5597, 2021.

[4] T. H. Jin et al., "Time-of-Arrival Measurement Using Adaptive CMOS IR-UWB Range Finder with Scalable Resolution," ***IEEE Tran. on Circuits and Systems-I***, Vol. 63, No. 10, pp. 1605-1615, Oct. 2016.

[5] Y. Kim et al., "Novel Chest Compression Depth Measurement Sensor Using IR-UWB for Improving Quality of Cardiopulmonary Resuscitation," ***IEEE Sensors J.***, Vol. 17, No. 10, pp. 3174-3183, May 2017.

[6] M. -J. Lee, W. -Y. Choi, "Effects of Parasitic Resistance on the Performance of Silicon APDs in Standard CMOS Technology," ***IEEE Electron Device Letters***, Vol. 37, No. 1, pp. 60~63, Jan. 2016.

[7] C. Hermans et al., "A high-speed 850-nm optical receiver front-end in 0.18-μm CMOS," ***IEEE J. Solid-State Circuits***, Vol. 41, No. 7, pp. 1606–1614, Jul. 2006.

[8] J. -E. Joo et al., "A CMOS Optoelectronic Receiver IC with an On-Chip Avalanche Photodiode for Home-Monitoring LiDAR Sensors," ***Sensors***, vol. 21, no. 13, pp. 4364, 2021.

Ji-Eun Joo received the B.S. and MSc degrees in electronic and electrical engineering from Ewha Womans University, Korea, in 2020 and 2022. Her current research interests include silicon photonics, and CMOS optoelectronic integrated circuits and architectures for short distance optical application systems and sensor interface IC designs.

Yu Hu received the B.S. degree in electrical engineering and automation from Anqing Normal University, Anqing, China, in 2016, and the M.S. degree from Ewha Womans University in 2023. Her current research interests include silicon photonics, and CMOS optoelectronic integrated circuits and architectures for short distance optical application systems and sensor interface IC designs.

Myung-Jae Lee received the B.S., M.S., and Ph.D. degrees in electrical and electronic engineering from Yonsei University, Seoul, South Korea, in 2006, 2008, and 2013, respectively. From 2013 to 2017, he was a Postdoctoral Researcher with the faculty of electrical engineering, Delft University of Technology (TU Delft), Delft, The Netherlands, and in 2017, he joined the school of engineering, École Polytechnique Fédérale de Lausanne (EPFL), Neuchâtel, Switzerland, as a Scientist. Since 2019, he has been a Senior Research Scientist with the Post-Silicon Semiconductor Institute, Korea Institute of Science and Technology (KIST), Seoul, South Korea, where he has led the research and development of next-generation single-photon detectors and sensors for various applications. His research interests include CMOS-compatible avalanche photodetectors and single-photon avalanche diodes and applications thereof.

Sung Min Park received the B.S. degree in electrical and electronic engineering from KAIST, Korea, in 1993. He received the M.S. degree in electrical engineering from University College London, U.K., in 1994, and the Ph.D. degree in electrical and electronic engineering from Imperial College London, U.K., in May 2000. In 2004, he joined the faculty of the Department of Electronics Engineering at Ewha Womans University, Seoul, Korea, where he is currently a Professor.